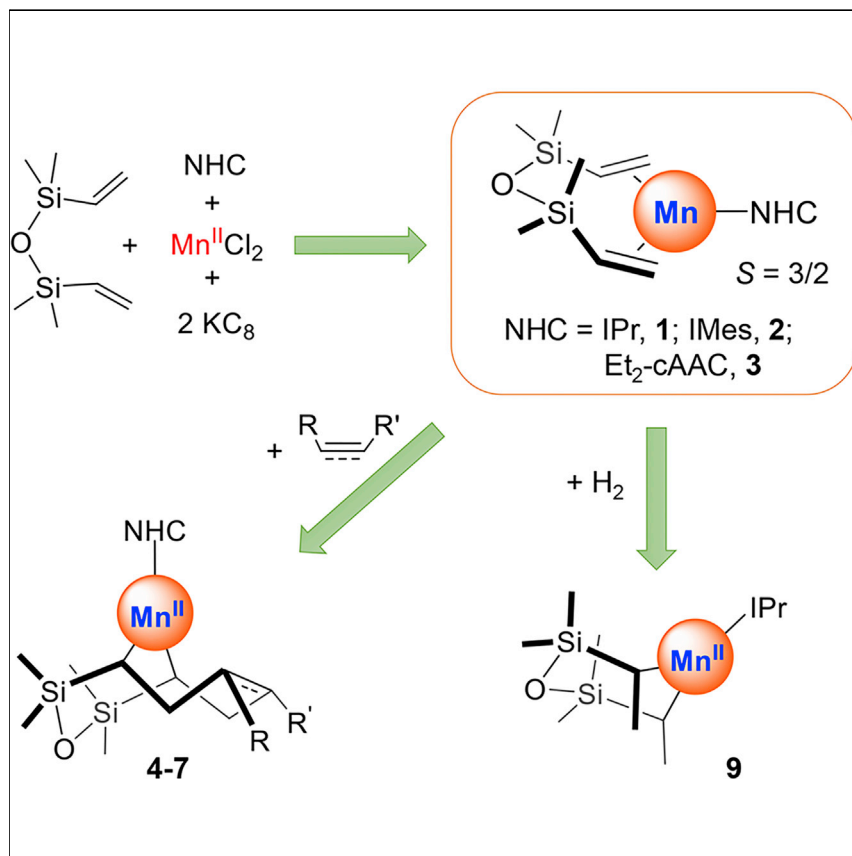


Article

The Stabilization of Three-Coordinate Formal Mn(0) Complex with NHC and Alkene Ligation



We report three-coordinate formal Mn(0) complexes $[(\text{NHC})\text{Mn}(\text{dvtms})]$ that have an $S = 3/2$ ground-spin state and feature highly covalent metal-ligand bonding. These complexes can perform reductive coupling with unsaturated hydrocarbons and show diversified reactivity toward H_2O , H_2 , CO , and I_2 . The results highlight the synthetic utility of low-coordinate low-valent manganese complexes, warranting further exploration.

Jun Cheng, Qi Chen, Xuebing
Leng, Zhongwen Ouyang,
Zhenxing Wang, Shengfa Ye,
Liang Deng

zxwang@hust.edu.cn (Z.W.)
shengfa.ye@kofo.mpg.de (S.Y.)
deng@sioc.ac.cn (L.D.)

HIGHLIGHTS

Three-coordinate formal Mn(0) complexes have been isolated

$S = 3/2$ ground-spin state and strong metal-to-alkene π backdonation

A rare example of Mn-mediated reductive coupling of unsaturated hydrocarbons

H_2 activation by low-coordinate formal Mn(0) alkene complex

Article

The Stabilization of Three-Coordinate Formal Mn(0) Complex with NHC and Alkene Ligation

Jun Cheng,¹ Qi Chen,¹ Xuebing Leng,¹ Zhongwen Ouyang,³ Zhenxing Wang,^{3,*} Shengfa Ye,^{2,*} and Liang Deng^{1,4,*}

SUMMARY

Low-coordinate zero-valent metal species are implicated as key intermediates in various transition-metal-catalyzed and -mediated reactions. However, knowledge on this type of metal species has been mainly restricted to the metals in groups 8–10, and that on the earlier transition-metal analogs is very limited. Herein, we report three-coordinate formal Mn(0) complexes $[(\text{NHC})\text{Mn}(\eta^2:\eta^2\text{-dvtms})]$ (NHC = *N*-heterocyclic carbene, dvtms = divinyltetramethyldisiloxane). Spectroscopic and computational studies established that these formal Mn(0) complexes have an $S = 3/2$ ground-spin state and feature strong metal-to-alkene π backdonation. As a result of the high covalency of the metal-ligand bonding, these formal Mn(0) complexes are best described as resonance among a series of limiting canonical structures of Mn(0)-dvtms, Mn(II)-[dvtm]²⁻, and Mn(IV)-[dvtms]⁴⁻. These formal Mn(0) complexes can perform reductive coupling with unsaturated hydrocarbons and show diversified reactivity toward H_2O , H_2 , CO , and I_2 , which hint at the synthetic utility of the three-coordinate formal Mn(0) species.

INTRODUCTION

Low-valent transition-metal species that simultaneously have low coordination numbers are important reactive intermediates proposed in many transition-metal-catalyzed reactions.^{1–3} This type of metal complex also shows intriguing reactivity in the activation of small molecules, e.g., H_2 , N_2 , CO , and CO_2 .^{4–11} Recently, low-coordinate low-valent 3d metal complexes were found to exhibit peculiar magnetic properties that imply their potential usage as new magnetic materials.^{12–19} Associated with these fascinating chemical and physical properties are their unusual electronic and geometric features, which in turn pose a great challenge to synthetic chemists.^{2,3,20–23} The inherent difficulty in preparing low-coordinate low-valent transition-metal complexes likely lies in the proneness of low-coordinate metal species to bind ligands to achieve coordination saturation and the readiness of low-valent metal species to undergo oxidative addition reactions because of their reduction potency. In this regard, one could reason that, among the metals in the same row of the periodic table, low-coordinate low-valent early transition-metal complexes should be highly reactive and could be more challenging to access than their late transition-metal analogs.

This perception seems to gain support from the status quo of the accessibility of low-coordinate zero-valent 3d metal complexes. Plenty of low-coordinate Ni(0), Co(0), and Fe(0) complexes featuring phosphine, *N*-heterocyclic carbene (NHC), and

The Bigger Picture

Low-coordinate zero-valent transition-metal species are a class of organometallic compounds that can mediate chemical bond activation and also be used as catalysts and starting materials for the synthesis of new organic and coordination compounds. Among versatile transition metals in the periodical table, low-coordinate zero-valent manganese complexes have long been sought after. However, because of their high chemical activity, these species are not easily accessed, and fundamental understanding of their properties is limited. Herein, we report the stabilization of three-coordinate formal zero-valent manganese complexes through the use of *N*-heterocyclic carbene and alkene ligands. The study also reveals the intriguing reactivity of this type of reactive metal species in mediating alkene transformation and dihydrogen activation.

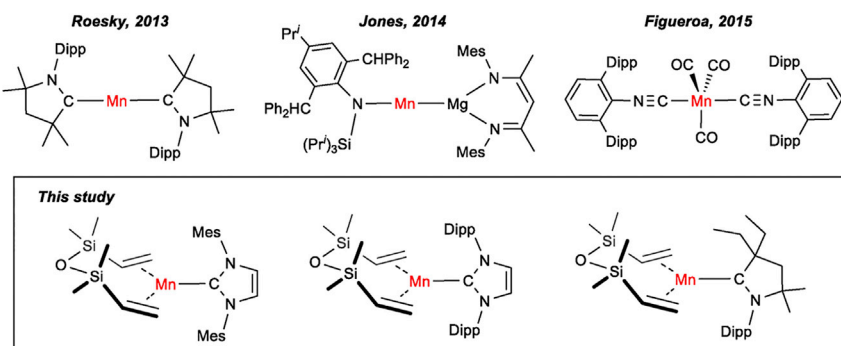


Figure 1. Examples of Highly Reactive Formal Mn(0) Complexes

isocyanide ligands have been reported.^{24–45} In contrast, isolable low-coordinate zero-valent transition-metal complexes of the earlier groups (groups 4–7), even for the ones with a formal oxidation state of zero, are rare. In 2013, Roesky et al. published a two-coordinate manganese complex supported by a cyclic aminoalkyl carbene (cAAC) ligand $[\text{Mn}(\text{Me}_2\text{-cAAC})_2]$ (Figure 1).⁴⁶ Its isolation apparently benefits from the strong π -accepting capability of cAAC. Spectroscopic and theoretical studies indicated that the pronounced Mn-to-cAAC backdonation endowed the Mn(I) or even Mn(II) nature of this formal Mn(0) complex. Consequently, the cAAC ligand possesses somewhat radical anion character, and the interaction of $[\text{Mn}(\text{Me}_2\text{-cAAC})_2]$ with H_2 causes the conversion of the cAAC ligands into alkyl ligands. In 2014, Jones reported another two-coordinate formal Mn(0) complex $[(^{\text{Mes}}\text{nacnac})\text{MgMn}(\text{N}(\text{C}_6\text{H}_2\text{-2,6-(CHPh}_2\text{-4-Pr')})(\text{SiPr}'_3))]$ (Figure 1) prepared from the reaction of the Mn(II) complex $[\text{MnBr}(\text{THF})(\text{N}(\text{C}_6\text{H}_2\text{-2,6-(CHPh}_2\text{-4-Pr')})(\text{SiPr}'_3))]_2$ with the Mg(I) dimer $[\text{Mg}(^{\text{Mes}}\text{nacnac})_2]$ ($^{\text{Mes}}\text{nacnac} = [(\text{MesNCMe})_2\text{CH}]^{1-}$).⁴⁷ This manganese complex features a unique Mn–Mg bond, and can be viewed as either a Mn(0)-Mg(II), Mn(I)-Mg(I), or Mn(II)-Mg(0) species. It reacts with Mn(II) and Cr(II) halides to form dinuclear Mn–Mn and Mn–Cr complexes, respectively, and its interactions with N_2O and $\text{Pr'}\text{NCNPr}'$ resulted in two-electron reduction of the substrates. Isolable five-coordinate $17e^-$ Mn(0) species are equally hard to access. Early studies found that $17e^-$ species $\text{Mn}(\text{CO})_5$ and $\text{Mn}(\text{CO})_3(\text{PR}_3)_2$ could be generated from photochemical substitution of dinuclear manganese complexes $[\text{Mn}_2(\text{CO})_8\text{L}_2]$ ($\text{L} = \text{CO}$, phosphine) but are hard to isolate because of their high activity.^{48–51} A recent study by Figueroa and co-workers showed that the use of sterically encumbering isocyanide ligands allows preparation and isolation of $17e^-$ species $[\text{Mn}(\text{CO})_3(\text{CNAr}')_2]$ ($\text{Ar}' = 2,6\text{-}(2',6'\text{-diisopropylphenyl})\text{phenyl}$, Figure 1).^{52,53} The metalloradical species displays intriguing reactivity of one-electron redox reactions to convert to Mn(I) and Mn(–I) complexes. Relevant to this, Chirik and co-workers reported a five-coordinate complex, $[(^{\text{IPr}}\text{PDI})\text{Mn}(\text{THF})_2]$ ($^{\text{IPr}}\text{PDI} = 2,6\text{-}(2',6'\text{-Pr}_2\text{C}_6\text{H}_3\text{N=CMe})_2\text{C}_5\text{H}_3\text{N}$).⁵⁴ Spectroscopic studies indicated that the electronic structure of its $S = 3/2$ ground-spin state was best formulated as a high-spin Mn(II) center antiferromagnetically coupled to a bis(imino)pyridine triplet diradical.

The limited knowledge on low-coordinate zero-valent 3d metal complexes of the metals in groups 4–7 urges further exploration. Toward this end, we wish to report the synthesis, characterization, and reactivity of the first three-coordinate formal zero-valent group 7 metal complexes $[(\text{NHC})\text{Mn}(\eta^2\text{:}\eta^2\text{-dvtms})]$ ($\text{NHC} = \text{IPr}$, 1; IMes, 2; Et₂-cAAC, 3; dvtms = divinyltetramethylidiloxane). Complexes 1–3 were prepared from one-pot reactions of MnCl_2 with NHC, dvtms, and KC_8 . Spectroscopic studies and theoretical calculations reveal an $S = 3/2$ ground-spin state for these

¹State Key Laboratory of Organometallic Chemistry, Center for Excellence in Molecular Synthesis, Shanghai Institute of Organic Chemistry, University of Chinese Academy of Sciences, Chinese Academy of Sciences, 345 Lingling Road, Shanghai 200032, P.R. China

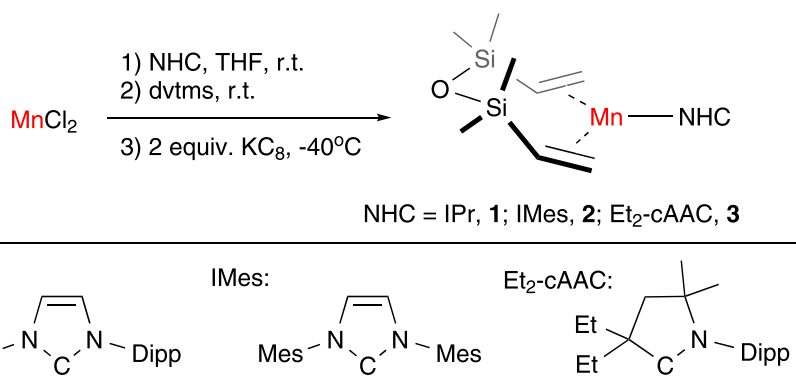
²Max-Planck Institut für Kohlenforschung, Kaiser-Wilhelm-Platz 1, 45470 Mülheim an der Ruhr, Germany

³Wuhan National High Magnetic Field Center & School of Physics, Huazhong University of Science and Technology, Wuhan 430074, P.R. China

⁴Lead Contact

*Correspondence: zxwang@hust.edu.cn (Z.W.), shengfa.ye@kofo.mpg.de (S.Y.), deng@sio.ac.cn (L.D.)

<https://doi.org/10.1016/j.chempr.2018.09.002>



Scheme 1. Preparation Route for the Formal Mn(0) Complexes **1–3**

formal Mn(0) complexes that feature highly covalent metal-ligand bonding arising from pronounced metal-to-alkene π backdonation. Consequently, the electronic structure of these formal Mn(0) complexes is best described as intermediate among several limiting canonical forms ranging from Mn(0) to Mn(IV). The formal Mn(0) complexes can facilitate reductive coupling of their dvtms ligand with alkene, allene, and alkyne to form seven-membered mangana(II) cycles, which represents a rare example of such transformations promoted by well-defined manganese complexes. The dvtms ligand in **1** can also be protonated by H₂O and partially hydrogenated by H₂. In addition, release of dvtms was observed when **1** was treated with I₂ or CO. These findings demonstrate the capability of the combined ligand set of NHC with vinylsilanes to stabilize low-coordinate formal zero-valent transition-metal complexes besides late transition metals and highlights the synthetic utility of low-coordinate NHC-Mn-alkene complexes.

RESULTS AND DISCUSSION

Synthesis and Characterization of the Three-Coordinate Formal Mn(0) Complexes

Low-valent manganese complexes are mostly known for five- and six-coordinate Mn(–I), Mn(0), and Mn(I) complexes with CO, isocyanide, cyclopentadienyl, and phosphine ligands,^{50–53,55–59} and low-valent manganese complexes with the lower coordination numbers of 2–4 are rare.^{16,17,46,47,60–63} Noting this and also the success of a combined ligand set of NHC with the bis(alkene) ligand dvtms in stabilizing three-coordinate Pt(0),⁶⁴ Pd(0),⁶⁵ Ni(0),^{31,32} Co(0),^{35–38} and Fe(0)^{39,41} complexes reported by Markó, Beller, Hazari, Johnson and co-workers, and us, we were curious whether this ligand set could allow stabilization of three-coordinate formal Mn(0) species or not. To our delight, our exploration proved its effectiveness.

Treatment of MnCl₂ with 1 equiv of the free NHC ligand (IPr, IMes, or Et₂-cAAC) in tetrahydrofuran (THF), followed by addition of 1 equiv of dvtms and 2 equiv of KC₈ at –40°C, gave deep brown mixtures. After workup and recrystallization, low-coordinate manganese complexes [(NHC)Mn(η^2 : η^2 -dvtms)] (NHC = IPr, **1**; IMes, **2**; Et₂-cAAC, **3**) were isolated in good yields (62%, 41%, and 65%, respectively) as crystalline solids from the mixtures (**Scheme 1**). The synthetic protocol is identical to that used for the preparation of the analogous formal Fe(0) and Co(0) complexes,^{35–39,41} but the reduction step has to be run at a low temperature (–40°C) as the trials to synthesize **1** at room temperature gave oily material that resisted crystallization. The failure suggests the high activity of the low-coordinate manganese species. With the aim of accessing similar low-coordinate manganese complexes bearing other alkene ligands, the reduction reactions of MnCl₂ with IPr and KC₈ in the presence of trimethylsilylethylene, isoprene, and diallyl

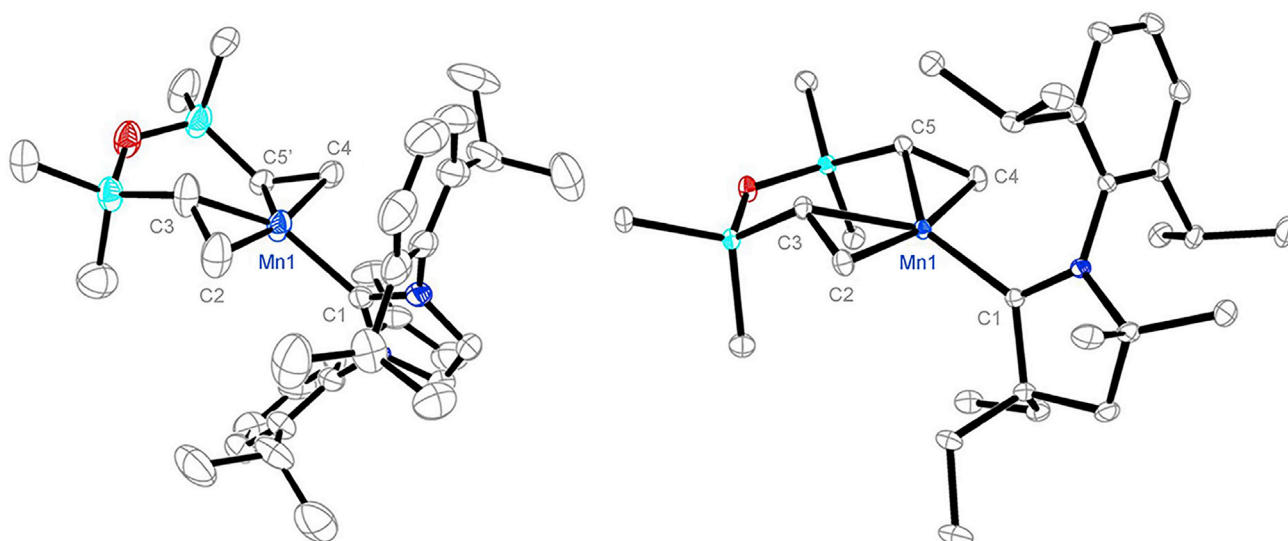


Figure 2. Molecular Structures of 1 and 3

Molecular structures of 1 (anti-isomer, left) and 3 (right) show 30% probability ellipsoids and the partial atom numbering scheme. Hydrogen atoms are omitted for clarity. Selected distances (\AA) and angles (deg) for 1 (anti-isomer): Mn1-C1 2.086(4), Mn1-C2 2.087(6), Mn1-C3 2.092(5), Mn1-C4 2.086(4), Mn1-C5' 2.106(7), C2-C3 1.382(8), C4-C5' 1.432(10), C1-Mn1-C2 97.0(2), C1-Mn1-C4 93.32(17), C2-Mn1-C3 38.6(2), C4-Mn1-C5' 40.0(3); for 3: Mn1-C1 2.0274(11), Mn1-C2 2.1320(11), Mn1-C3 2.1165(11), Mn1-C4 2.1010(11), Mn1-C5 2.1155(11), C2-C3 1.4322(16), C4-C5 1.4319(16), C1-Mn1-C2 91.29(4), C1-Mn1-C4 100.00(4), C2-Mn1-C3 39.40(4), C4-Mn1-C5 39.70(4).

ether were examined. Unfortunately, these reactions produced brown oily mixtures from which no desired manganese complex could be isolated.

As isolated, 1 and 2 present as green solids, and 3 is red. They are soluble in toluene, diethyl ether, and THF, and slightly soluble in *n*-hexane. Complexes 1–3 are air and moisture sensitive; however, they show good stability in both solid state and solution when stored under a nitrogen atmosphere and at -30°C . Complexes 1–3 have been characterized by ^1H NMR (Figures S11–S13), superconducting quantum interference device (SQUID) measurement (Figure 3; see also Figure S42), electron paramagnetic resonance (EPR) spectroscopy (Figures 4 and 5; see also Figure S43), absorption spectroscopy (Figure S6), elemental analysis, and single-crystal X-ray diffraction study (Figure 2; see also Figure S1 and Data S1 and S2). Consistent with their different color, the absorption spectra of 1 and 2 in THF feature two absorption bands at ca. 400 and 660 nm, whereas two bands at the maxima of 480 and 705 nm with large absorption coefficients were observed in the spectrum of 3 (Figure S6). The difference in the absorption spectra may arise from the different electronic nature of their carbene ligands.^{66,67} Complexes 1–3 are paramagnetic, as suggested by their ^1H NMR spectra measured in benzene- d_6 exhibiting heavily broadened, paramagnetically shifted signals in the range +20 to -30 ppm (Figures S11–S13). Solution magnetic susceptibility measurements (Evans method in benzene- d_6 at room temperature) indicated magnetic moments of 4.0, 3.9, and 3.7 μ_{B} for 1–3, respectively, which are close to the spin-only value of 3.87 μ_{B} for 3d ions with an $S = 3/2$ state.

Molecular Structures

The solid-state structures of 1 and 3 were established by single-crystal X-ray diffraction studies (Figure 2; see also Figure S1, Table S1, and Data S1 and S2). The manganese centers in both complexes are coordinated by one NHC ligand and one $\eta^2:\eta^2$ -dvtms ligand, forming a trigonal planar geometry. The Mn–C(carbene) bond distances in 1 and 3 are 2.086(4) and 2.027(2) \AA , respectively, which are shorter

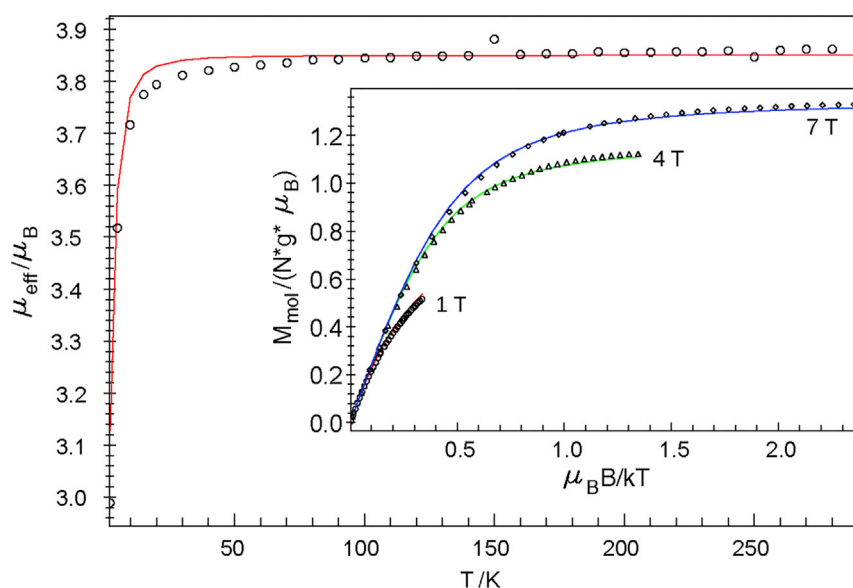


Figure 3. Magnetization Measurements of 3

Temperature dependence of the magnetic moment, μ_{eff} , of a solid sample of 3 recorded in a 1.0 T magnetic field and variable field and variable temperature dependence of the magnetization of 3 (inset). The solid lines represent best fits using the parameters given in the text.

than those of high-spin Mn(II) complexes $[\text{Mn}_2\text{Cl}_2(\mu\text{-Cl})_2(\text{iPr})_2]$ (2.183(5) and 2.196(5) Å),⁶⁸ $[(\text{iPr})\text{Mn}(\text{Mes})_2]$ (2.195(2) Å),⁶⁹ $[(\text{iPr})\text{Mn}(\text{CH}_2\text{SiMe}_3)_2]$ (2.236(2) Å),⁷⁰ $[(\text{iPr})\text{Mn}(\text{CH}(\text{SiMe}_3)_2)_2]$ (2.277(4) Å),⁷⁰ and also the Mn(II) dialkyl complexes 4–7 and 9 (2.177(8)–2.189(4) Å, see below). The contracted Mn–C(carbene) separations in 1 and 3 might be related to the high covalency of the Mn–C(carbene) bond in low-valent manganese complexes. Similar phenomena were also observed in low-coordinate iron- and cobalt-NHC complexes.^{35,39} The $\eta^2\cdot\eta^2$ -dvtms ligand in 1 is disordered and was modeled as a mixture of *syn*- and *anti*-isomers based on the relative alignment of the vinyl moieties. The *anti*-isomer has Mn–C(alkene) distances in a narrow range of 2.086(4)–2.106(7), and C(alkene)–C(alkene) distances of 1.382(8) and 1.432(10). These C(alkene)–C(alkene) bonds are distinctly longer than the C=C bonds in vinylsilanes (1.32 Å),⁷¹ indicating strong π backdonation from the formal Mn(0) center to the dvtms ligand. But they are comparable with those found for $[\text{CpCo}(\text{CH}_2\text{CHSiMe}_3)_2]$ (1.408(2) Å),⁷² $[(\text{dppe})\text{Fe}(\eta^2\cdot\eta^2\text{-dvtms})]$ (1.409(5) Å),⁷³ $[(\text{Cp}^*)_2\text{Ti}(\text{CH}_2\text{CH}_2)]$ (1.438(5) Å),⁷⁴ and $[\text{Ti}(\text{CH}_2\text{CH}_2)(\text{OAr}^*)_2(\text{PMe}_3)]$ (1.425(5) Å).⁷⁵ The titanium complexes are thought to be intermediate between the limiting electronic structures of Ti(II) ethylene and Ti(IV) metallacyclopropane. However, when compared with the corresponding C–C bonds in the metalla- and thia-cyclopropanes, $[(\text{PPh}_3)_2\text{Pt}(\text{trans-NCCHCH}_2\text{CN})]$ (1.53(4) Å),⁷⁶ $[\text{Cp}^*\text{Ta}(\text{CH}_2\text{CH}_2)(\text{CHBu}^*)(\text{PMe}_3)]$ (1.477(4) Å),⁷⁷ and thioethylene $\text{CH}_2\text{CH}_2\text{S}$ (1.484(3) Å),⁷⁸ the C(alkene)–C(alkene) distances in 1 are apparently shorter. Also, these C(alkene)–C(alkene) distances are longer than those in manganese complexes $[(\eta^5\text{-C}_5\text{H}_4(\text{CH}_3))\text{Mn}(\text{CO})(\text{C}_6\text{H}_5)(\eta^2\text{-NHCH}_2\text{CH=CH}_2)]$ (1.37(1) Å)⁷⁹ but close to that in $\text{Li}_4[\text{MnH}(\text{CH}_2\text{CH}_2)(\text{dmpe-H})_2]_2$ (1.41(1) Å).⁸⁰ In the crystal structure of 3, the $\eta^2\cdot\eta^2$ -dvtms ligand presents in a *syn* form. The Mn–C(alkene) distances also fall into a narrow range of 2.101(1)–2.132(1) Å, which are comparable with those in 1 and slightly shorter than the Mn(II)–C bonds in $[(\text{THF})_2\text{Mn}(1,3\text{-SiMe}_3)_2\text{C}_3\text{H}_3]$ (2.174(2) Å) and $[(\text{tmida})\text{Mn}(1,1',3\text{-SiMe}_3)_3\text{C}_3\text{H}_2]_2$ (2.189(3) Å).⁸¹ The C(alkene)–C(alkene) distance (1.432(2) Å) of 3 is comparable with those in 1. Thus, among these structure data,

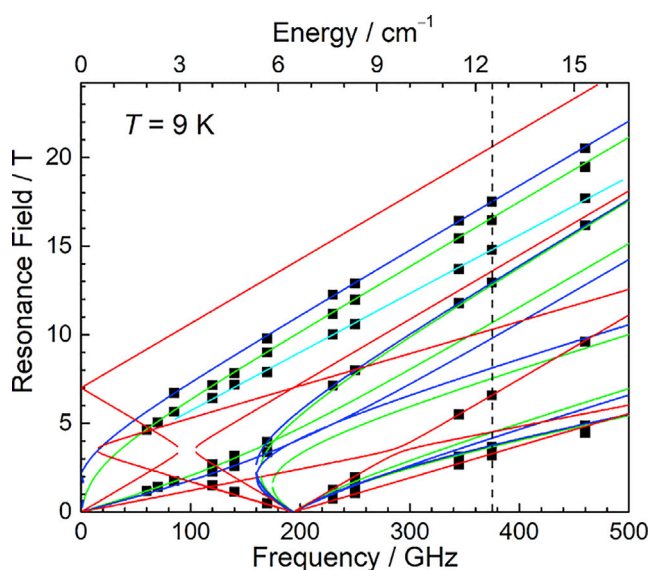


Figure 4. Resonance Field versus Microwave Frequency (Quantum Energy) of EPR Transitions for 3

The Hamiltonian parameters used are: $S = 3/2$, $g_x = 1.97(2)$, $g_y = 1.97(2)$, $g_z = 1.97(2)$, $|D| = 3.22(3)$ cm $^{-1}$, $E = 0.14(3)$ cm $^{-1}$. Green, blue, and red curves are the simulations using the best-fitted spin Hamiltonian parameters with the magnetic field H parallel to the x , y , and z axes of the ZFS tensor, respectively. The vertical dashed line represents the frequency (375 GHz) used in Figure 5 at which the spectra were recorded or simulated.

The C(alkene)–C(alkene) distances in 1 and 3 indicate strong backdonation from their formal Mn(0) center to the dvtms ligand, but the backdonation is not strong enough to allow the assignment of these complexes as manganacyclop propane s.

The accessibility of 1–3 proved the effectiveness of the combined ligand set of NHC with dvtms in stabilizing zero-valent metal complexes besides late transition metals. Comparison of the structures of a series of formal zero-valent metal complexes involving different metal centers, $[(\text{NHC})\text{M}(\eta^2:\eta^2\text{-dvtms})]$ ($\text{M} = \text{Ni, Co, Fe, Mn}$; NHC = IMes or IPr)^{32,35,39} showed a stepwise increase in the M–C(carbene) distances from 1.91 to 1.95 to 2.03 and to 2.09 Å upon going from Ni to Co to Fe and to Mn. In parallel, the M–C(alkene) bonds also gradually lengthen (Table S4). Both observations thus reveal the overwhelming effect of the differential atomic radii of the elements from Ni to Co to Fe and to Mn that largely dictates the variation of the metal–ligand bond distances. Despite the subtle structure change, the detailed electronic interaction between the dvtms ligand and the metal center in the series of complexes (NHC)M(dvtms) could be different. Interestingly, irrespective of the metal center in $[(\text{NHC})\text{M}(\eta^2:\eta^2\text{-dvtms})]$, the C(alkene)–C(alkene) bond lengths are nearly identical. This reflects the strong reduction potency of Mn(0) over the zero-valent late 3d transition metals, because 1 has the longest M–C(alkene) bond distances.

Electronic Structure of the Three-Coordinate Formal Mn(0) Complexes

Noting the rarity of low-coordinate formal Mn(0) complexes, spectroscopic characterization and theoretical studies on 1 and 3 have been performed to probe their electronic structures. Because analogous results were found for both complexes, we focus our discussion on 3 (Figures 3, 4, 5, and 6; see also Figures S43 and S44) and summarize the data for 1 (Figures S42, S45, and S46) in the Supplemental Information.

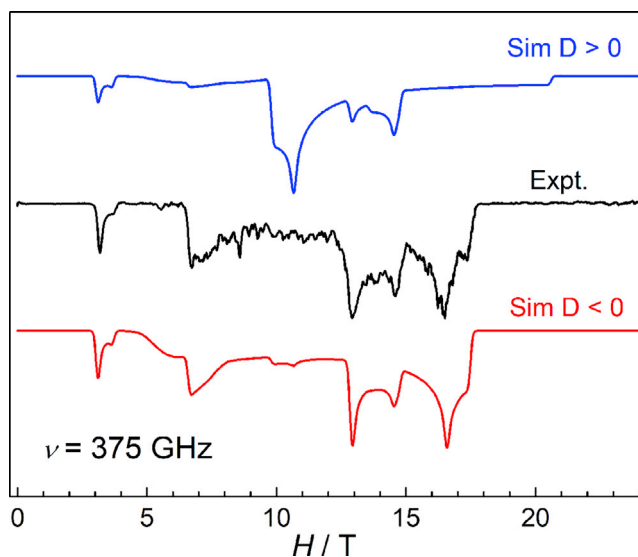


Figure 5. High-Frequency EPR Spectrum of 3 with Its Simulations at 375 GHz and 9 K

The blue trace represents the spectrum simulated using the positive D value, for which the magnitude is determined in Figure 4. The red trace is the spectrum simulated using the corresponding negative D value. The other Hamiltonian parameters used are the same as those in Figure 4.

From variable temperature (2–295 K) magnetic susceptibility and variable temperature and variable-field magnetization measurements (Figure 3), a quartet ground state ($S = 3/2$) has been established for 3. The solid line in Figure 3 represents a simulation using the usual $S = 3/2$ spin Hamiltonian (Equation 1) with $g_{\text{iso}} = 1.99(1)$, $D = -3.8(1) \text{ cm}^{-1}$, $E/D = 0.04(2)$, and temperature-independent paramagnetism = 10×10^{-6} electromagnetic units (emu). Here, D and E are the axial and rhombic zero-field splitting (ZFS) parameters, and g is the intrinsic g matrix.

$$\hat{H} = D \left[\hat{S}_z^2 - \frac{1}{3} S(S+1) + \frac{E}{D} (\hat{S}_x^2 - \hat{S}_y^2) \right] + \beta \vec{B} \cdot \vec{g} \hat{S} \quad (\text{Equation 1})$$

The high-frequency (HF)-EPR experiments on the polycrystalline powder samples of 3 were carried out at 9 K and various frequencies to accurately determine the spin Hamiltonian parameters. The results are plotted in Figure 4 as the field dependence of the resonances on the frequencies. Obviously, one of the zero-field transitions is observed at about 6.4 cm^{-1} . This corresponds to the effective splitting $2|D'|$ ($D' = \sqrt{D^2 + 3E^2}$) between the two Kramers doublets of a quartet state ($S = 3/2$). A least-square fit to a complete two-dimensional array of the resonances yields the following parameters: $g_x = 1.97(2)$, $g_y = 1.97(2)$, $g_z = 1.97(2)$, $|D| = 3.22(3) \text{ cm}^{-1}$, and $E = 0.14(3) \text{ cm}^{-1}$, which are in reasonable agreement with those determined by the magnetization and X-band EPR studies ($|D| = 3.5\text{--}3.8 \text{ cm}^{-1}$) supplied in the [Supplemental Information](#). To confirm the sign of D , a single-frequency spectrum (375 GHz) was simulated as shown in Figure 5, which confirms the negative sign of D ($D = -3.22(3) \text{ cm}^{-1}$).

To gain further insights into the nature of 3, we have undertaken detailed computational investigations using a wavefunction-based multireference completely active space self-consistent field (CASSCF) approach. To this end, an active space consisting of 7 electrons distributed into 12 orbitals was chosen. In addition to the five Mn 3d and two dvtms C=C π^* orbitals, the Mn 4d shell was also included in the active space to account for double-shell effects.^{82,83} To lower the computational cost, a truncated model (3'), in which the Dipp and Et substituents in the carbene ligand were replaced by Ph and Me, was used. Figure 6 depicts the resulting natural orbitals

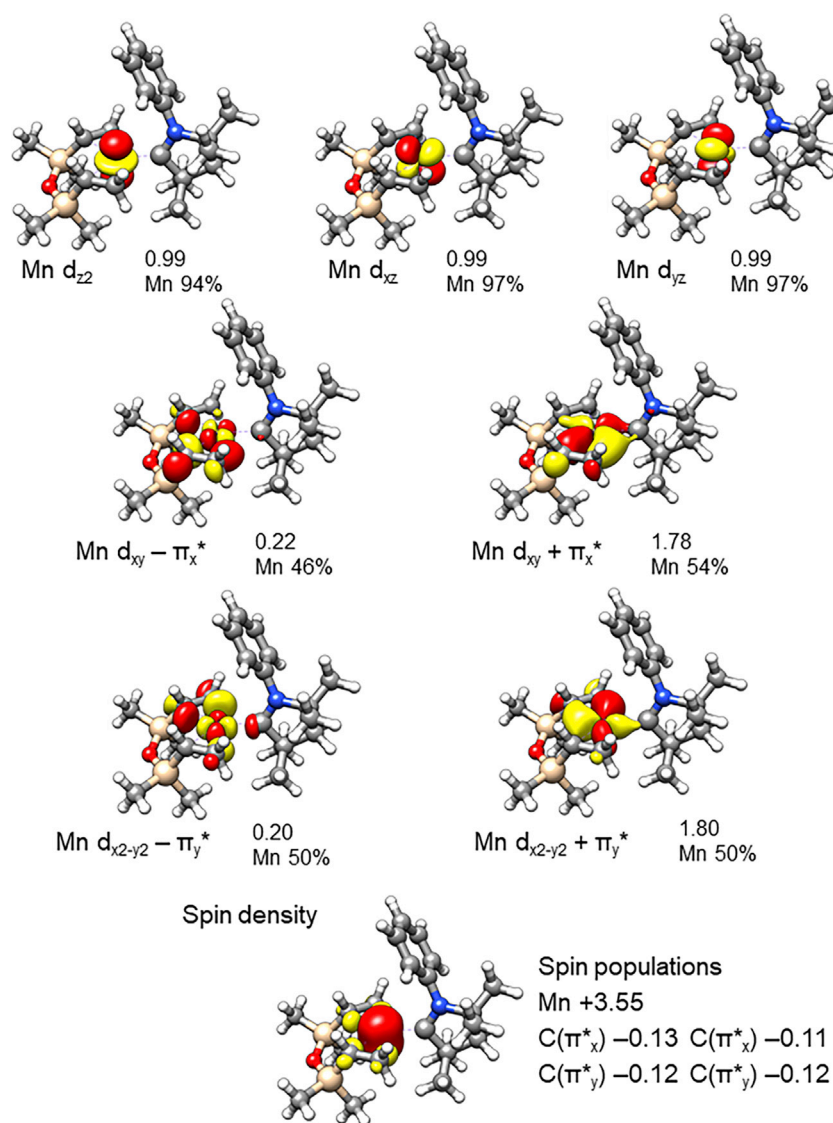


Figure 6. Natural Orbitals of 3' Derived from the Ground-State CASSCF(7,12) Calculations

The occupation number along with the dominant atomic contribution is indicated near each orbital.

derived from the ground-state CASSCF(7,12) calculations. One can identify three singly occupied, essentially nonbonding orbitals of predominant Mn 3d parentage (d_{z2} , d_{xz} , and d_{yz}) and strong π backdonation from the Mn d_{xy} and d_{x2-y2} orbitals to the dvtms C=C π^* orbitals, as demonstrated by two pairs of the bonding and antibonding combinations labeled as Mn $d_{xy/x2-y2} + \pi_{x/y}^*$ and Mn $d_{xy/x2-y2} - \pi_{x/y}^*$, respectively. In a simplified picture, the π backdonation in 3' can be interpreted as electron transfer from a formal Mn(0) center to the dvtms ligand via two channels, each involving two electrons. This process would eventually lead to formation of a formal Mn(IV) center and a tetra-anionic ligand ([dvtms] $^{4-}$), once it was completely finished. The CASSCF(7,12) wavefunction of 3' has a principal electron configuration of $(d_{xy} + \pi_x^*)^2(d_{x2-y2} + \pi_y^*)^2(d_{z2})^1(d_{xz})^1(d_{yz})^1(d_{xy} - \pi_x^*)^0(d_{x2-y2} - \pi_y^*)^0$ with a weight of 73%, and none of the remaining electron configurations has a weight exceeding 7%. Notably, the non-negligible negative spin population (~0.25) found for each π bond of dvtms is substantially lower than 1 as expected for a C=C π^* radical

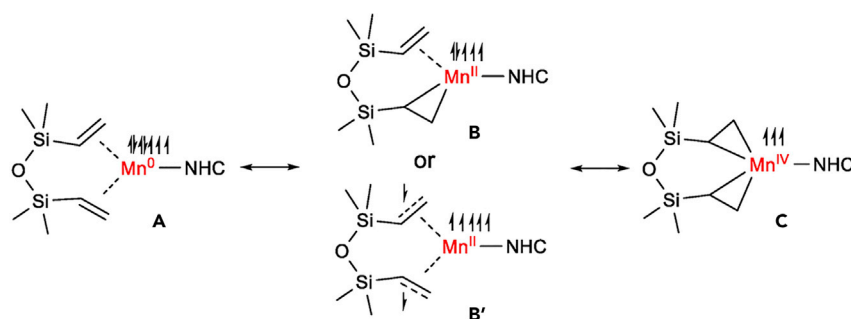


Figure 7. Canonical Forms of the Low-Coordinate Manganese Species at an $S = 3/2$ State

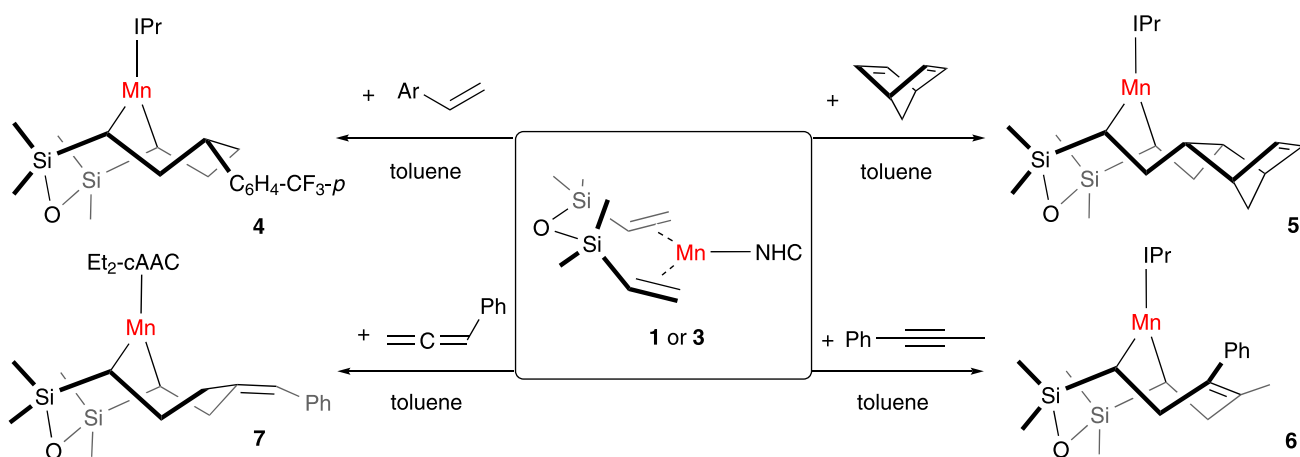
The half arrows on Mn and alkene moieties denote the 3d and unpaired 2p electrons, respectively.

(Figure 6). Thus, the negative spin density in dvtms mainly arises from spin polarization, for which the α - and β -electron transfers from the doubly occupied d_{xy/x^2-y^2} orbitals of a formal Mn(0) center cannot take place simultaneously.^{84,85} The nearly identical contributions of the Mn d_{xy} and $d_{x^2-y^2}$ atomic orbitals and the dvtms C=C π^* orbitals in Mn $d_{xy/x^2-y^2} + \pi_{x/y}^*$ and Mn $d_{xy/x^2-y^2} - \pi_{x/y}^*$ indicate almost the highest degree of metal-ligand covalency that renders unambiguous assignment of the physical oxidation state of the metal center difficult.⁸⁶ It has been reported that under such circumstances, attempts to assign the physical oxidation state using X-ray absorption spectroscopy fail as well.^{87,88} Therefore, the bonding of 3 has to be interpreted as resonance among a series of limiting canonical electronic structures of a high-spin Mn(0) center ($S_{\text{Mn}} = 3/2$) ligated by a dvtms ligand (A in Figure 7), an intermediate-spin Mn(II) ion ($S_{\text{Mn}} = 3/2$) bound to a dianionic ligand ($[\text{dvtms}]^{2-}$) (B in Figure 7), a high-spin Mn(II) ($S_{\text{Mn}} = 5/2$) antiferromagnetically coupled to a triplet dianionic ligand ($[\text{dvtms}]^{\cdot-2-}$) ($S_{\text{dvtms}} = 1$) yielding an overall quartet state ($S_{\text{total}} = 3/2$) (B' in Figure 7), and a high-spin Mn(IV) ion ($S_{\text{Mn}} = 3/2$) chelated by a tetra-anionic ligand ($[\text{dvtms}]^4-$) (C in Figure 7). Such highly covalent metal-ligand interactions were encountered in our earlier study, and the electronic structures were also interpreted as resonance among several limiting bonding situations.⁸⁹ The B3LYP calculations of complex 3 also deliver a qualitatively identical bonding picture (Figure S44). As expected, 1 was also computed to feature the same electronic structure despite involving a different NHC ligand (Figures S45–S46). Thus, the calculations indicate that the high stability of these formal Mn(0) complexes (NHC) Mn(dvtms) apparently results from the good π -accepting nature of dvtms in addition to the sterically demanding and strong σ -donating nature of NHC.

Reactivity of the Three-Coordinate Formal Mn(0) Complexes

Complexes 1–3 are rare examples of low-coordinate formal Mn(0) alkene complexes. Given the limited knowledge on low-coordinate manganese alkene complexes, the growing interest in manganese-catalyzed organic transformations in recent years^{90–93} prompted us to perform a careful reactivity study on these manganese complexes.

These low-coordinate manganese complexes are found to be reactive toward alkenes, alkynes, and allenes. The reactions of 4-(trifluoromethyl)styrene, 2,5-norbornadiene, 1-phenyl-1-propyne, and phenyl allene with 1 or 3 occurred at room temperature, from which Mn(II) complexes bearing carbodianionic chelates 4–7 were isolated in high yields (Scheme 2). Single-crystal X-ray diffraction studies unambiguously established the structures of 4–7 as Mn(II) complexes (Figure 8; see also Figures S2 and S3, Tables S1 and S2, and Data S3, S4, S5, and S6) resulting from manganese-mediated reductive coupling of the two alkene moieties of the dvtms



Scheme 2. Reactions of the Formal Mn(0) Complexes with Alkene, Alkyne, and Allene

ligand in 1 or 3 with the added unsaturated hydrocarbons. As a representative, Figure 8 depicts the structures of 4 and 6. The unique manganabicyclo[4.3.1]decane frameworks in 4–7 contain metallacycloheptane rings. The ones in 4 and 7 adapt a twisted chair conformation, and those in 5 and 6 are in a boat conformation. The substituents, silyl, aryl, and alkyl groups, on the C(sp^3) atoms of the seven-membered manganacycles are all *cisoid* to each other. The observed stereospecificity might be traced back to the steric demanding nature of the NHC ligands, which renders the reductive coupling reactions stereoselective. Metallacycloheptanes are key intermediates in a plethora of transition-metal catalyzed coupling reactions of alkenes, and their isolation proved challenging due to their readiness to undergo β -hydride elimination.^{94–96} Considering this, the accessibility of 4–7 most likely reflects the unique steric feature of the poly-ring system that might prevent the manganese center from approaching the β -H atoms. Complexes 4–7 were further characterized by ^1H NMR (Figures S14–S18), solution magnetic susceptibility measurements, absorption spectroscopy (Figures S7 and S8), and elemental analysis. Their long Mn–C distances and large magnetic moments indicate their high-spin ($S = 5/2$) Mn(II) nature.

The reactions of the formal Mn(0) complexes with unsaturated hydrocarbons represent the first examples of reductive couplings of alkenes and alkynes mediated by well-defined manganese complexes. Such reactions are useful methods for C–C bond formation and are often promoted by low-valent transition-metal species of Ti, Zr, Cr, Fe, Ni, and Co.^{97–101} Probably because of the difficulty in accessing low-coordinate low-valent manganese species, manganese-mediated reductive coupling reactions have been rarely reported. To our knowledge, the coupling of norbornadiene with 1,3-butadiene catalyzed by the Ziegler-Natta catalyst $\text{Mn}(\text{acac})_2$ with Pr'MgCl or Et_3Al , which produced 3-vinylcyclo[4.2.1.0^{2,5}]non-7-ene and 5-(buta-1,3-dien-1-yl)bicyclo[2.2.1]hept-2-ene in low yields, is the only relevant example.¹⁰² To get more insight into this reductive coupling reaction, the influence of the electronic properties of the mono-alkene was examined by comparing the relative rates of the reactions of 1 with 4-trifluoromethylstyrene, styrene, and 4-methoxystyrene. The controlled reactions on NMR scale revealed that, while all the alkenes could react with 1 to afford similar reductive coupling products as suggested by their similar resultant ^1H NMR spectra (Figure S19), the reaction times required for complete conversion of 1 (6, 48, and 192 hr, respectively) are different. The enhanced rates of the reaction with electron-deficient alkenes are consistent with those of the reductive coupling reactions mediated by other transition metals and hints

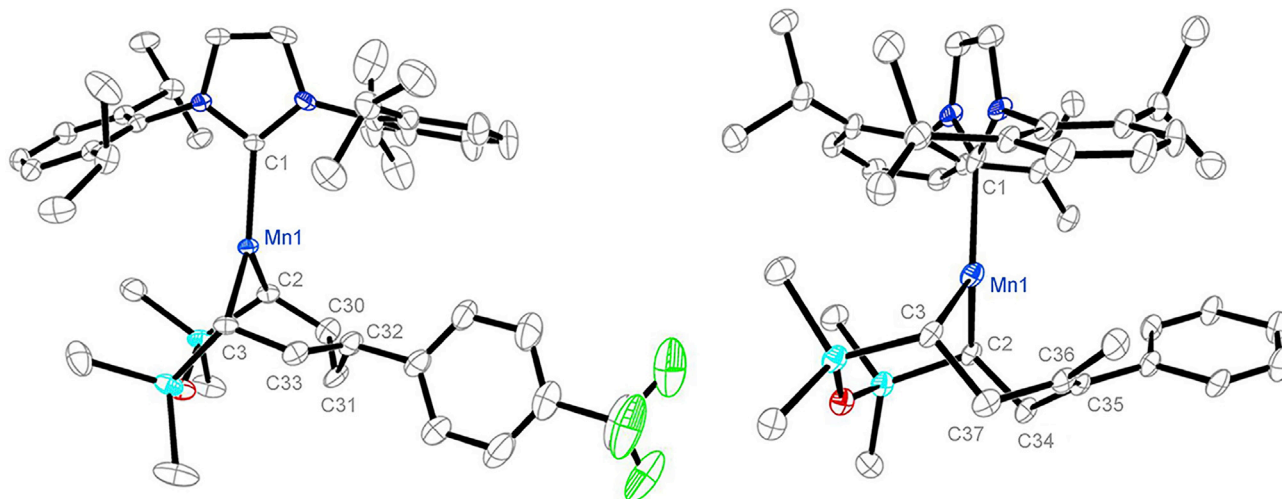
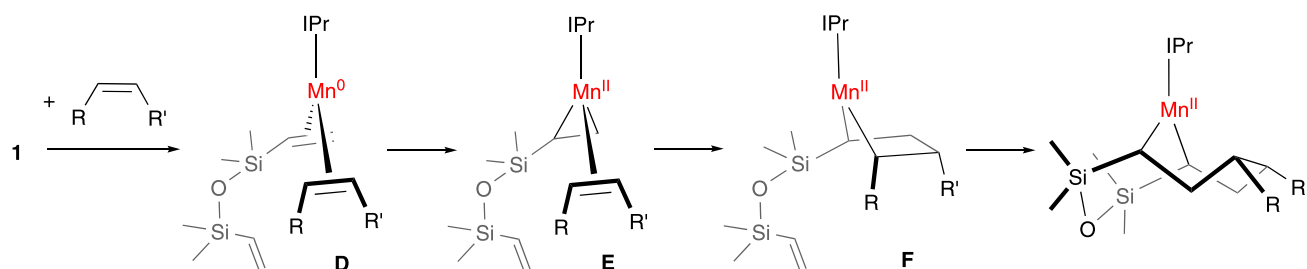


Figure 8. Molecular Structures of 4 and 6

Molecular structures of 4 (left) and 6 (right) show 30% probability ellipsoids and the partial atom numbering scheme. Hydrogen atoms are omitted for clarity. Selected distances (\AA) and angles (deg) for 4: Mn1-C1 2.189(4), Mn1-C2 2.153(5), Mn1-C3 2.140(5), C2-C30 1.535(7), C30-C31 1.552(8), C31-C32 1.535(8), C32-C33 1.544(7), C3-C33 1.547(7), C1-Mn1-C2 130.76(17), C1-Mn1-C3 124.68(16), C2-Mn1-C3 104.36(18); for 6: Mn1-C1 2.177(8), Mn1-C2 2.142(7), Mn1-C3 2.158(7), C2-C34 1.574(9), C34-C35 1.552(9), C3-C37 1.564(9), C36-C37 1.518(10), C35-C36 1.345(9), C1-Mn1-C2 134.3(2), C1-Mn1-C3 120.7(3), C2-Mn1-C3 102.6(3).

at the electron richness of the manganese species.^{97–101} Accordingly, the formation of 4–7 may be rationalized by a classic reductive coupling mechanism mediated by low-valent transition metals.^{97–101,103} As an example, Scheme 3 shows a feasible pathway for the reactions of 1 with alkenes. The reaction might start from the ligand-replacement reaction of one alkene moiety of the dvtrms ligand in 1 by the added alkene molecule, 4-(trifluoromethyl)styrene or 2,5-norbornadiene, which gives new bis(alkene) formal Mn(0) species D. Species D undergoes a reductive coupling reaction, presumably via manganacyclopropane intermediate E, to form manganacyclopentane F. Further insertion of the appended alkene moiety of F into its metallacyclopentane ring could eventually produce the manganacycloheptanes. In the C–C bond formation steps, the capability of the α -silyl group to stabilize carboanion,¹⁰⁴ steric repulsions imparted by the bulky NHC ligands, and ring constraints are among the key determinants that govern the regio- and stereoselectivity of the coupling reaction. Considering the different ground-spin state between 4–7 ($S = 5/2$) and 1 and 3 ($S = 3/2$), these reductive coupling reactions must involve a spin crossover.^{105,106} Whether the C–C bond formation steps occurring on the energy surface of $S = 3/2$ or $S = 5/2$ remains an open question. Thus, elucidating the reaction mechanism and addressing the above question needs a detailed experimental and theoretical mechanistic investigation.

The low-coordinate formal Mn(0) complexes also showed diversified reactivity toward H_2O , H_2 , I_2 , and CO . Hydrolysis of 1 with a large excess amount of H_2O at -78°C furnished mono-alkene $\text{EtMe}_2\text{SiOSiMe}_2\text{CH}=\text{CH}_2$ (8) in 92% NMR yield. Upon replacing H_2O by D_2O , the corresponding di-deuterium compound, $\text{CH}_2\text{DCHDSiMe}_2\text{OSiMe}_2\text{CH}=\text{CH}_2$ (8-d₂), was obtained in a high yield (Scheme 4). Compounds 8 and 8-d₂ were characterized by NMR (Figures S20–S28) and mass spectrometry. The deviation of the quantitative deuteration ratio of 8-d₂ could be due to the presence of a small amount of H_2O in deuterated water. In addition, the capability of low-coordinate low-valent transition-metal complexes in activating C–H bonds could also partly make a contribution.^{107,108} The formation of these mono-alkenes hints at the contribution of the mangana(II)-cyclopropane form (B in Figure 7) in the canonical structures of the three-coordinate formal Mn(0) alkene complexes.



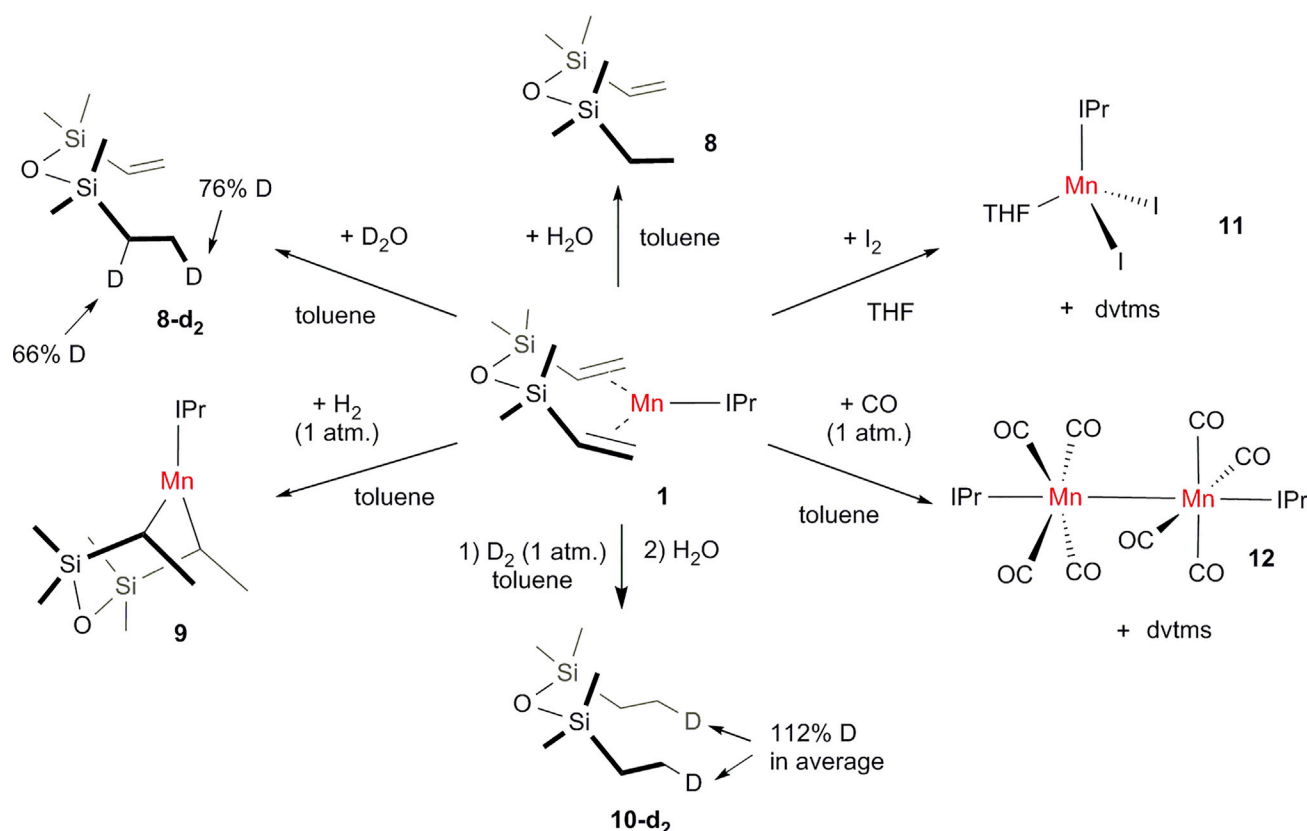
Scheme 3. Proposed Mechanism for the Manganese-Mediated Reductive Coupling Reactions of 1 with Alkenes

Complex 1 can also react with H₂ (1 atm) at room temperature to give a Mn(II) alkyl complex (9) in 71% yield (Scheme 4). The reaction presents rare examples of H₂ activation by low-valent manganese species. Precedents are only known for the reaction of photo-excited manganese atoms with H₂ in a cryogenic matrix¹⁰⁹ and the reaction of Roesky's [Mn(Me₂-cAAC)₂] with H₂.⁴⁶ Complex 9 has been characterized by ¹H NMR (Figure S29), UV-visible spectroscopy (Figures S7 and S8), solution magnetic susceptibility measurement, X-ray diffraction studies (Figure 9; see also Table S3 and Data S7), as well as elemental analysis. Comparing its structure with that of 1 revealed that the hydrogenation reaction resulted in addition of two hydrogen atoms to the two terminal carbon atoms of the alkene moieties of the dvtms ligand. Indeed, exposure of 1 to D₂ (1 atm.) in toluene followed by hydrolysis with H₂O led to the formation of (DCH₂CH₂(CH₃)₂Si)₂O (10-d₂) in a high yield (Scheme 4). The generation of 9 could be explained by a route starting from the σ-bond metathesis of 1 in form B with H₂ to yield manganese(II) alkyl hydride species, followed by migratory insertion (Scheme S1). Alternatively, the classic route involves oxidative addition of 1, in form A, with H₂ to afford Mn(II) species (IPr)MnH₂(dvtms) that undergoes further migratory insertion reactions to produce 9 (Scheme S1). Notably, as the combined ¹H, ²H, ¹³C, and ¹³C DEPT-135 NMR analysis (Figures S30–S38) indicate a high D incorporation in the methyl position of 10-d₂ (112%), the elementary steps in the proposed paths (Scheme S1) could be reversible. Complex 9 is unreactive toward H₂ (1 atm.) at room temperature, which might account for the unsuccessful attempt to perform catalytic hydrogenation of dvtms using 1 as the catalyst.

Different from the aforementioned reactions, the interactions of 1 with I₂ and CO did not lead to functionalization of dvtms, rather to its release. Treatment of 1 with 1 equiv of I₂ afforded the Mn(II) complex [(IPr)MnI₂(THF)] (11) and dvtms in high yields (Scheme 4). On the other hand, the exposure of 1 with an excess amount of CO (1 atm.) produced [(IPr)Mn(CO)₄]₂ (12) and dvtms (Scheme 4). Complexes 11 and 12 have been characterized by single-crystal X-ray diffraction analyses (Figures S4 and S5; see also Table S3 and Data S8 and S9), NMR (Figures S39–S41) and absorption spectroscopy (Figures S9 and S10). These reaction outcomes are distinct from the well-established reactivity of transition-metal alkyl complexes with I₂ and CO, wherein iodination and CO-insertion reactions usually occur.^{110,111} These reactions seem to be more congruent with the Mn(0)-alkene canonical form (A in Figure 7) of the formal Mn(0) alkene complexes.

Conclusion

In this study, we showed that the stabilization and isolation of low-coordinate formal Mn(0) species can be achieved through the use of a combined ligand set of monodentate NHC and dvtms and that the resultant manganese complexes [(NHC)Mn(dvtms)] have rich reactivity. The low-coordinate manganese complexes [(NHC)Mn(dvtms)] were readily prepared from the reactions of NHC with MnCl₂, dvtms,



Scheme 4. Reactions of 1 with H_2O , D_2O , H_2 , D_2 , I_2 , and CO

and KC_8 . They represent rare examples of isolable low-coordinate formal zero-valent transition-metal complexes besides known late transition-metal complexes. Spectroscopic characterization in combination with theoretical studies revealed their $S = 3/2$ ground-spin state and strong π backdonation from the metal centers to the alkene moieties. As a result of the high covalency of the metal-ligand interaction, these formal Mn(0) complexes are better interpreted as intermediate between a series of limiting canonical structures of Mn(0), Mn(II), and Mn(IV). In accord with the electronic nature, $[(\text{NHC})\text{Mn}(\text{dvtms})]$ exhibits intriguing reactivity of reductive coupling with alkenes and alkynes to form Mn(II) dialkyl complexes, which is unprecedented for manganese complexes. In addition, $[(\text{NHC})\text{Mn}(\text{dvtms})]$ can react with H_2O to give mono-alkene $\text{EtMe}_2\text{SiOSiMe}_2\text{CH}=\text{CH}_2$, can be hydrogenated by H_2 to form Mn(II) dialkyl compound, can be oxidized by I_2 to give Mn(II) diiodide, and can also undergo a ligand-substitution reaction with CO to form a Mn(0) carbonyl complex. In the latter two reactions, the dvtms ligand was released without further conversion. These results highlight the synthetic utility of low-coordinate low-valent manganese complexes, which warrants further exploration.

EXPERIMENTAL PROCEDURES

Full experimental procedures are provided in the [Supplemental Information](#).

DATA AND SOFTWARE AVAILABILITY

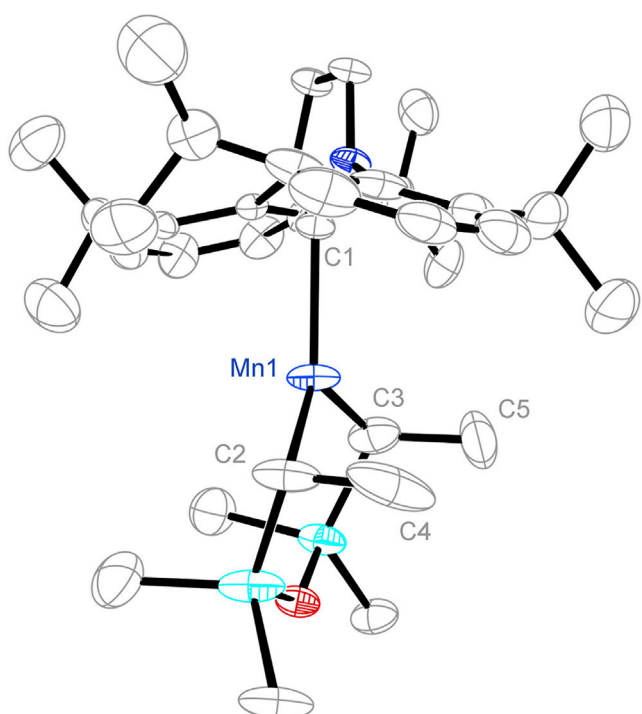


Figure 9. Molecular Structure of 9

Molecular structure of **9** shows 30% probability ellipsoids and the partial atom numbering scheme. Hydrogen atoms are omitted for clarity. Selected distances (\AA) and angles (deg): Mn1-C1 2.181(5), Mn1-C2 2.129(7), Mn1-C3 2.148(9), C2-C4 1.601(16), C3-C5 1.572(14), C1-Mn1-C2 127.8(2), C1-Mn1-C3 115.2(3), C2-Mn1-C3 115.2(3).

CCDC: 1845539, 1845540, 1845541, 1845542, 1845543, 1845544, 1845545, 1845546, and 1845547, respectively.

SUPPLEMENTAL INFORMATION

Supplemental Information includes Supplemental Experimental Procedures, 46 figures, 1 scheme, 4 tables, and 9 data files and can be found with this article online at <https://doi.org/10.1016/j.chempr.2018.09.002>.

ACKNOWLEDGMENTS

The work was supported by the National Key Research and Development Program (2016YFA0202900), the National Natural Science Foundation of China (21725104, 21690062, and 21432001), and the Strategic Priority Research Program of the Chinese Academy of Sciences (XDB20000000). S.Y. gratefully acknowledges the financial support from the Max Planck Society. We are deeply indebted to Dr. Eckhard Bill for fruitful discussions and to Mr. Andreas Göbel for SQUID measurements.

AUTHOR CONTRIBUTIONS

Investigation, J.C., S.Y., and L.D.; Synthetic Studies, J.C. and Q.C.; Crystallographic Studies, X.L.; EPR Experiments, S.Y., Z.O., and Z.W.; SQUID Experiments, S.Y.; Computational Experiments, S.Y.; Writing – Original Draft, J.C., Z.W., S.Y., and L.D.; Writing – Review & Editing, Z.W., S.Y., and L.D.; Supervision, L.D.

DECLARATION OF INTERESTS

The authors declare no competing interests.

Received: May 28, 2018

Revised: July 30, 2018

Accepted: September 10, 2018

Published: October 4, 2018

REFERENCES AND NOTES

1. Beller, M., and Bolm, C. (2004). Transition Metals for Organic Synthesis: Building Blocks and Fine Chemicals (Wiley-VCH).
2. Ellis, J.E. (2006). Adventures with substances containing metals in negative oxidation states. *Inorg. Chem.* 45, 3167–3186.
3. Power, P.P. (2012). Stable two-coordinate, open-shell (d_1-d_9) transition metal complexes. *Chem. Rev.* 112, 3482–3507.
4. Lin, T.P., and Peters, J.C. (2013). Boryl-mediated reversible H₂ activation at cobalt: catalytic hydrogenation, dehydrogenation, and transfer hydrogenation. *J. Am. Chem. Soc.* 135, 15310–15313.
5. Laplaza, C.E., and Cummins, C.C. (1995). Dinitrogen cleavage by a three-coordinate molybdenum(III) complex. *Science* 268, 861–863.
6. Rodriguez, M.M., Bill, E., Brennessel, W.W., and Holland, P.L. (2011). N₂ reduction and hydrogenation to ammonia by a molecular iron-potassium complex. *Science* 334, 780–783.
7. Suess, D.L.M., and Peters, J.C. (2013). A CO-derived iron dicarbyne that releases olefin upon hydrogenation. *J. Am. Chem. Soc.* 135, 12580–12583.
8. Gao, Y.F., Li, G.Y., and Deng, L. (2018). Bis(dinitrogen)cobalt(-1) complexes with NHC ligation: synthesis, characterization, and their dinitrogen functionalization reactions affording side-on bound diazene complexes. *J. Am. Chem. Soc.* 140, 2239–2250.
9. Buss, J.A., and Agapie, T. (2016). Four-electron deoxygenative reductive coupling of carbon monoxide at a single metal site. *Nature* 529, 72–75.
10. Sadique, A.R., Brennessel, W.W., and Holland, P.L. (2008). Reduction of CO₂ to CO using low-coordinate iron: formation of a four-coordinate iron dicarbonyl complex and a bridging carbonate complex. *Inorg. Chem.* 47, 784–786.
11. Yeung, C.S., and Dong, V.M. (2008). Beyond Aresta's complex: Ni- and Pd-catalyzed organozinc coupling with CO₂. *J. Am. Chem. Soc.* 130, 7826–7827.
12. Zadrozny, J.M., Xiao, D.J., Atanasov, M., Long, G.J., Grandjean, F., Neese, F., and Long, J.R. (2013). Magnetic blocking in a linear iron(I) complex. *Nat. Chem.* 5, 577–581.
13. Atanasov, M., Zadrozny, J.M., Long, J.R., and Neese, F. (2013). A theoretical analysis of chemical bonding, vibronic coupling, and magnetic anisotropy in linear iron(II) complexes with single-molecule magnet behavior. *Chem. Sci.* 4, 139–156.
14. Meng, Y.S., Mo, Z.B., Wang, B.W., Zhang, Y.Q., Deng, L., and Gao, S. (2015). Observation of the single-ion magnet behavior of d⁸ ions on two-coordinate Co(I)-NHC complexes. *Chem. Sci.* 6, 7156–7162.
15. Bryan, A.M., Merrill, W.A., Reiff, W.M., Fettinger, J.C., and Power, P.P. (2012). Synthesis, Structural, and magnetic characterization of linear and bent geometry cobalt(II) and nickel(II) amido complexes: evidence of very large spin-orbit coupling effects in rigorously linear coordinated Co²⁺. *Inorg. Chem.* 51, 3366–3373.
16. Lin, C.Y., Fettinger, J.C., Chilton, N.F., Formanuk, A., Grandjean, F., Long, G.J., and Power, P.P. (2015). Salts of the two-coordinate homoleptic manganese(I) dialkyl anion [Mn(C(SiMe₃)₃)₂]⁻ with quenched orbital magnetism. *Chem. Commun.* 51, 13275–13278.
17. Werncke, C.G., Suturina, E., Bunting, P.C., Vendier, L., Long, J.R., Atanasov, M., Neese, F., Sabo-Etienne, S., and Bontemps, S. (2016). Homoleptic two-coordinate silylamido complexes of chromium(I), manganese(I), and cobalt(I). *Chem. Eur. J.* 22, 1668–1674.
18. Werncke, C.G., Bunting, P.C., Duhayon, C., Long, J.R., Bontemps, S., and Sabo-Etienne, S. (2015). Two-coordinate iron(I) complex [Fe{N(SiMe₃)₂}₂]⁻: synthesis, properties, and redox activity. *Angew. Chem. Int. Ed.* 54, 245–248.
19. Danopoulos, A.A., Braunstein, P., Monakhov, K.Y., van Leusen, J., Kögerler, P., Clémancey, M., Latour, J.M., Benayad, A., Tromp, M., Rezabal, E., et al. (2017). Heteroleptic, two-coordinate [M(NHC){N(SiMe₃)₂}]⁻ (M = Co, Fe) complexes: synthesis, reactivity and magnetism rationalized by an unexpected metal oxidation state. *Dalton Trans.* 46, 1163–1171.
20. Bradley, D.C., and Chisholm, M.H. (1976). Transition-metal dialkylamides and disilylamides. *Acc. Chem. Res.* 9, 273–280.
21. Cummins, C.C. (1998). Three-coordinate complexes of "hard" ligands: advances in synthesis, structure and reactivity. *Prog. Inorg. Chem.* 47, 685–836.
22. Holland, P.L. (2008). Electronic structure and reactivity of three-coordinate iron complexes. *Acc. Chem. Res.* 41, 905–914.
23. Roy, S., Mondal, K.C., and Roesky, H.W. (2016). Cyclic alkyl(amino) carbene stabilized complexes with low coordinate metals of enduring nature. *Acc. Chem. Res.* 49, 357–369.
24. Caddick, S., Cloke, F.G.N., Hitchcock, P.B., and Lewis, A.K.D. (2004). Unusual reactivity of a nickel N-heterocyclic carbene complex: tert-butyl group cleavage and silicone grease activation. *Angew. Chem. Int. Ed.* 43, 5824–5827.
25. Danopoulos, A.A., and Pugh, D. (2008). A method for the synthesis of nickel(0) bis(carbene) complexes. *Dalton Trans.* 30–31.
26. Mondal, K.C., Samuel, P.P., Li, Y., Roesky, H.W., Roy, S., Ackermann, L., Sidhu, N.S., Sheldrick, G.M., Carl, E., Demeshko, S., et al. (2014). A catalyst with two-coordinate nickel: theoretical and catalytic studies. *Eur. J. Inorg. Chem.* 2014, 818–823.
27. Krüger, C., and Tsay, Y. (1972). Molecular and crystal-structure of bis(ethylene)(tricyclohexylphosphine)nickel. *J. Organomet. Chem.* 34, 387–395.
28. Jolly, P.W., Krüger, C., Salz, R., and Wilke, G. (1976). Preparation and structure of (divinylcyclohexene)-nickel-phosphine complexes. *J. Organomet. Chem.* 118, C25–C27.
29. Pörschke, K., Wilke, G., and Krüger, C. (1983). Lithiumcarbamoyl-bis(ethene)nickel(0). *Angew. Chem. Int. Ed.* 22, 547–548.
30. Bair, J.S., Schramm, Y., Sergeev, A.G., Clot, E., Eisenstein, O., and Hartwig, J.F. (2014). Linear-selective hydroarylation of unactivated terminal and internal olefins with trifluoromethyl-substituted arenes. *J. Am. Chem. Soc.* 136, 13098–13101.
31. Elsby, M.R., and Johnson, S.A. (2017). Nickel-catalyzed C–H silylation of arenes with vinylsilanes: rapid and reversible β-Si elimination. *J. Am. Chem. Soc.* 139, 9401–9407.
32. Wu, J.G., Faller, J.W., Hazari, N., and Schmeier, T.J. (2012). Stoichiometric and catalytic reactions of thermally stable nickel(0) NHC complexes. *Organometallics* 31, 806–809.
33. Laskowski, C.A., Miller, A.J.M., Hillhouse, G.L., and Cundari, T.R. (2011). A two-coordinate nickel imido complex that effects C–H amination. *J. Am. Chem. Soc.* 133, 771–773.
34. Ung, G., Rittle, J., Soleilhavoup, M., Bertrand, G., and Peters, J.C. (2014). Two-coordinate Fe⁰ and Co⁰ complexes supported by cyclic (alkyl)(amino) carbenes. *Angew. Chem. Int. Ed.* 53, 8427–8431.
35. Zhang, L., Liu, Y.S., and Deng, L. (2014). Three-coordinate cobalt(IV) and cobalt(V) imido

- complexes with N-heterocyclic carbene ligation: synthesis, structure, and their distinct reactivity in C-H bond amination. *J. Am. Chem. Soc.* 136, 15525–15528.
36. Du, J.Z., Wang, L.B., Xie, M.H., and Deng, L. (2015). A two-coordinate cobalt(II) imido complex with NHC ligation: synthesis, structure, and reactivity. *Angew. Chem. Int. Ed.* 54, 12640–12644.
37. Yao, X.N., Du, J.Z., Zhang, Y.Q., Leng, X.B., Yang, M.W., Jiang, S.D., Wang, Z.X., Ouyang, Z.W., Deng, L., Wang, B.W., et al. (2017). Two-coordinate Co(II) imido complexes as outstanding single molecule magnets. *J. Am. Chem. Soc.* 139, 373–380.
38. Sun, J., Gao, Y.F., and Deng, L. (2017). Low-coordinate NHC-cobalt(0)-olefin complexes: synthesis, structure, and their reactions with hydrosilanes. *Inorg. Chem.* 56, 10775–10784.
39. Zhang, H.Z., Ouyang, Z.W., Liu, Y.S., Zhang, Q., Wang, L., and Deng, L. (2014). (Aminocarbene)(divinyltetramethyldisiloxane) iron(0) compounds: a class of low-coordinate iron(0) reagents. *Angew. Chem. Int. Ed.* 53, 8432–8436.
40. Ung, G., and Peters, J.C. (2015). Low-temperature N₂ binding to two-coordinate L₂Fe⁰ enables reductive trapping of L₂FeN₂⁻ and NH₃ generation. *Angew. Chem. Int. Ed.* 54, 532–535.
41. Wang, L., Hu, L.R., Zhang, H.Z., Chen, H., and Deng, L. (2015). Three-coordinate iron(IV) bisimido complexes with aminocarbene ligation: synthesis, structure, and reactivity. *J. Am. Chem. Soc.* 137, 14196–14207.
42. Barnett, B.R., and Figueira, J.S. (2016). Zero-valent isocyanides of nickel, palladium and platinum as transition metal σ-type Lewis bases. *Chem. Commun.* 52, 13829–13839.
43. Emerich, B.M., Moore, C.E., Fox, B.J., Rheingold, A.L., and Figueira, J.S. (2011). Protecting-group-free access to a three-coordinate nickel(0) tris-isocyanide. *Organometallics* 30, 2598–2608.
44. Fox, B.J., Millard, M.D., DiPasquale, A.G., Rheingold, A.L., and Figueira, J.S. (2009). Thallium(I) as a coordination site protection agent: preparation of an isolable zero-valent nickel tris-isocyanide. *Angew. Chem. Int. Ed.* 48, 3473–3477.
45. Margulieux, G.W., Weidemann, N., Lacy, D.C., Moore, C.E., Rheingold, A.L., and Figueira, J.S. (2010). Isocyan analogues of [Co(CO)₄]⁰: a tetraisocyanide of cobalt isolated in three states of charge. *J. Am. Chem. Soc.* 132, 5033–5035.
46. Samuel, P.P., Mondal, K.C., Roesky, H.W., Hermann, M., Frenking, G., Demeshko, S., Meyer, F., Stückl, A.C., Christian, J.H., Dalal, N.S., et al. (2013). Synthesis and characterization of a two-coordinate manganese complex and its reaction with molecular hydrogen at room temperature. *Angew. Chem. Int. Ed.* 52, 11817–11821.
47. Hicks, J., Hoyer, C.E., Moubaraki, B., Li Manni, G., Carter, E., Murphy, D.M., Murray, K.S., Gagliardi, L., and Jones, C. (2014). A two-coordinate manganese(0) complex with an unsupported Mn-Mg bond: allowing access to low coordinate homo- and heterobimetallic compounds. *J. Am. Chem. Soc.* 136, 5283–5286.
48. Kidd, D.R., and Brown, T.L. (1978). Photochemical substitution-reactions of Mn₂(CO)₁₀. *J. Am. Chem. Soc.* 100, 4095–4103.
49. Kidd, D.R., Cheng, C.P., and Brown, T.L. (1978). Formation and properties of substituted manganese carbonyl radicals. *J. Am. Chem. Soc.* 100, 4103–4107.
50. McCullen, S.B., and Brown, T.L. (1982). Preparation, properties, and kinetics of the reaction with tributyltin hydride of manganese(0) radicals Mn(CO)₃(R₃P)₂. *J. Am. Chem. Soc.* 104, 7496–7500.
51. McCullen, S.B., Walker, H.W., and Brown, T.L. (1982). Direct observation of substitution-reactions of tricarbonylbis(phosphine) manganese(0) radicals. *J. Am. Chem. Soc.* 104, 4007–4008.
52. Agnew, D.W., Moore, C.E., Rheingold, A.L., and Figueira, J.S. (2015). Kinetic destabilization of metal-metal single bonds: isolation of a pentacoordinate manganese(0) monoradical. *Angew. Chem. Int. Ed.* 54, 12673–12677.
53. Agnew, D.W., Sampson, M.D., Moore, C.E., Rheingold, A.L., Kubiak, C.P., and Figueira, J.S. (2016). Electrochemical properties and CO₂-reduction ability of m-terphenyl isocyanide supported manganese tricarbonyl complexes. *Inorg. Chem.* 55, 12400–12408.
54. Russell, S.K., Bowman, A.C., Lobkovsky, E., Wieghardt, K., and Chirik, P.J. (2012). Synthesis and electronic structure of reduced Bis(imino)pyridine manganese compounds. *Eur. J. Inorg. Chem.* 2012, 535–545.
55. Treichel, P.M. (1982). Volume 4: manganese. In *Comprehensive Organometallic Chemistry*, G. Wilkinson, F.G.A. Stone, and E.W. Abel, eds. (Pergamon), pp. 1–159.
56. Aspinall, H.C., and Deeming, A.J. (1985). The addition of protic acids to [Mn₂(CO)₅(Ph₂PCH₂PPh₂)₂] to give bridging hydrido-compounds. *J. Chem. Soc. Dalton Trans.* 743–747.
57. Hartl, F., Mahabiersing, T., Floch, P.L., Mathey, F., Ricard, L., Rosa, P., and Záliš, S. (2003). Electronic properties of 4,4',5,5'-tetramethyl-2,2'-biphosphinine (tmbp) in the redox series Fac-[Mn(Br)(CO)₃(tmbp)], [Mn(CO)₃(tmbp)]₂, and [Mn(CO)₃(tmbp)]: crystallographic, spectroelectrochemical, and DFT computational study. *Inorg. Chem.* 42, 4442–4455.
58. Lemke, F.R., and Kubiak, C.P. (1985). Photochemistry of a novel asymmetrically diphosphine-bridged binuclear manganese(0) complex - mer, fac-Mn₂(CO)₆(Me₂PCH₂PM₂)₂. *J. Chem. Soc. Chem. Commun.* 1729–1730.
59. Xue, Z.L., Wang, Y.M., Mack, J., Zhu, W.H., and Ou, Z.P. (2015). Synthesis, characterization, and electrochemistry of the manganese(I) complexes of meso-substituted [14]trienzotriphyrins(2.1.1). *Chem. Eur. J.* 21, 2045–2051.
60. Chai, J.F., Zhu, H.P., Stückl, A.C., Roesky, H.W., Magull, J., Bencini, A., Caneschi, A., and Gatteschi, D. (2005). Synthesis and reaction of [{HC(CMeNAr)₂}Mn]₂ (Ar=2,6-iPr₂C₆H₃): the complex containing three-coordinate manganese(I) with a Mn-Mn bond exhibiting unusual magnetic properties and electronic structure. *J. Am. Chem. Soc.* 127, 9201–9206.
61. Fohlemeister, L., Liu, S.S., Schulter, C., Moubaraki, B., Stasch, A., Cashion, J.D., Murray, K.S., Gagliardi, L., and Jones, C. (2012). Low-coordinate iron(I) and manganese(I) dimers: kinetic stabilization of an exceptionally short Fe-Fe multiple bond. *Angew. Chem. Int. Ed.* 51, 8294–8298.
62. Lu, D.Y., Yu, J.S.K., Kuo, T.S., Lee, G.H., Wang, Y., and Tsai, Y.C. (2011). Theory-guided experiments on the mechanistic elucidation of the reduction of dinuclear zinc, manganese, and cadmium complexes. *Angew. Chem. Int. Ed.* 50, 7611–7615.
63. Sorace, L., Golze, C., Gatteschi, D., Bencini, A., Roesky, H.W., Chai, J., and Stuckl, A.C. (2006). Low-valent low-coordinated manganese(I) ion dimer: a temperature dependent W-band EPR study. *Inorg. Chem.* 45, 395–400.
64. Markó, I.E., Stérin, S., Buisine, O., Mignani, G., Branlard, P., Tinant, B., and Declercq, J.P. (2002). Selective and efficient platinum(0)-carbene complexes as hydrosilylation catalysts. *Science* 298, 204–206.
65. Jackstell, R., Harkal, S., Jiao, H.J., Spannenberg, A., Borgmann, C., Rottger, D., Nierlich, F., Elliot, M., Niven, S., Cavell, K.J., et al. (2004). An industrially viable catalyst system for palladium-catalyzed telomerizations of 1,3-butadiene with alcohols. *Chem. Eur. J.* 10, 3891–3900.
66. Hahn, F.E., and Jahnke, M.C. (2008). Heterocyclic carbenes: synthesis and coordination chemistry. *Angew. Chem. Int. Ed.* 47, 3122–3172.
67. Melaimi, M., Jazzar, R., Soleilhavoup, M., and Bertrand, G. (2017). Cyclic (alkyl)(amino) carbenes (CAACs): recent developments. *Angew. Chem. Int. Ed.* 56, 10046–10068.
68. Al-Afyouni, M.H., Krishnan, V.M., Arman, H.D., and Tonzeitich, Z.J. (2015). Synthesis and reactivity of manganese(II) complexes containing n-heterocyclic carbene ligands. *Organometallics* 34, 5088–5094.
69. Musgrave, R.A., Turberville, R.S.P., Irwin, M., and Goicoechea, J.M. (2012). Transition metal complexes of anionic N-heterocyclic dicarbene ligands. *Angew. Chem. Int. Ed.* 51, 10832–10835.
70. Kennedy, A.R., Klett, J., Mulvey, R.E., and Robertson, S.D. (2011). N-heterocyclic-carbene-induced monomerization of sterically encumbered dialkylmagnesium and dialkylmanganese polymers. *Eur. J. Inorg. Chem.* 2011, 4675–4679.
71. Bruña, S., González-Vadillo, A.M., Nieto, D., Pastor, C., and Cuadrado, I. (2010). Vinyl-functionalized silanes and disiloxanes with electronically communicated ferrocenyl units. *Organometallics* 29, 2796–2807.
72. Hapke, M., Weding, N., and Spannenberg, A. (2010). Highly reactive cyclopentadienylcobalt(I) olefin complexes. *Organometallics* 29, 4298–4304.

73. Burcher, B., Sanders, K.J., Benda, L., Pintacuda, G., Jeanneau, E., Danopoulos, A.A., Braunstein, P., Olivier-Bourbigou, H., and Breuil, P.A.R. (2017). Straightforward access to stable, 16-valence-electron phosphine-stabilized Fe^0 Olefin complexes and their reactivity. *Organometallics* 36, 605–613.
74. Cohen, S.A., Auburn, P.R., and Bercaw, J.E. (1983). Structure and reactivity of bis(pentamethylcyclopentadienyl)(ethylene) titanium(II), a simple olefin adduct of titanium. *J. Am. Chem. Soc.* 105, 1136–1143.
75. Hill, J.E., Fanwick, P.E., and Rothwell, I.P. (1992). Synthesis, structure, and reactivity of a new series of titanium η^2 -olefin and η^2 -ketone complexes. *Organometallics* 11, 1771–1773.
76. Panattoni, C., Graziani, R., Bandoli, G., Clemente, D.A., and Belluco, U. (1970). Crystal and molecular structure of fumaronitrilebis(triphenylphosphine)-platinum. *J. Chem. Soc. B*, 371–377.
77. Schultz, A.J., Brown, R.K., Williams, J.M., and Schrock, R.R. (1981). Low-temperature neutron-diffraction studies of C-H-metal interactions in two tantalum-neopentylidene complexes: $[\text{Ta}(\text{CHCM}\text{e}_3)(\text{PM}\text{e}_3)\text{Cl}_3]_2$ [$T = 110\text{K}$] and the first alkylidene/olefin complex, $\text{Ta}(\eta^5\text{-C}_5\text{M}\text{e}_5)(\text{CHCM}\text{e}_3)(\eta^2\text{-C}_2\text{H}_4)(\text{PM}\text{e}_3)$ [$T = 20\text{K}$]. *J. Am. Chem. Soc.* 103, 169–176.
78. Okiye, K., Hirose, C., Lister, D.G., and Sheridan, J. (1974). The r_s -structure of ethylene sulfide. *Chem. Phys. Lett.* 24, 111–113.
79. Mcgeary, M.J., Tonker, T.L., and Templeton, J.L. (1985). Synthesis and structure of a chelated manganese carbene-alkene complex. *Organometallics* 4, 2102–2106.
80. Girolami, G.S., Howard, C.G., Wilkinson, G., Dawes, H.M., Thorntonpett, M., Motevalli, M., and Hursthouse, M.B. (1985). Alkyl, hydrido, and tetrahydroaluminato complexes of manganese with 1,2-bis(dimethylphosphino)ethane (dmpe) - x-ray crystal-structures of $\text{Mn}_2(\mu\text{-C}_2\text{H}_{11})_2(\text{C}_6\text{H}_{11})_2(\mu\text{-dmpe})$, $(\text{dmpe})_2\text{Mn}(\mu\text{-H})_2\text{AlH}(\mu\text{-H})_2\text{AlH}(\mu\text{-H})_2\text{Mn}(\text{dmpe})_2$, and $\text{Li}_4(\text{MnH}(\text{C}_2\text{H}_4)[\text{CH}_2(\text{Me})\text{PCH}_2\text{CH}_2\text{PM}\text{e}_2]_2)_2\text{ZEt}_2\text{O}$. *J. Chem. Soc. Dalton Trans.* 921–929.
81. Engerer, L.K., Carlson, C.N., Hanusa, T.P., Brennessel, W.W., and Young, V.G. (2012). σ -Vs π -bonding in manganese(II) allyl complexes. *Organometallics* 31, 6131–6138.
82. Jannuzzi, S.A.V., Phung, Q.M., Domingo, A., Formiga, A.L.B., and Pierloot, K. (2016). Spin state energetics and oxyl character of Mn-oxo porphyrins by multiconfigurational ab initio calculations: implications on reactivity. *Inorg. Chem.* 55, 5168–5179.
83. Alcover-Fortuny, G., Caballol, R., Pierloot, K., and de Graaf, C. (2016). Role of the imide axial ligand in the spin and oxidation state of manganese corrole and corrolazine complexes. *Inorg. Chem.* 55, 5274–5280.
84. Kupper, C., Mondal, B., Serrano-Plana, J., Klawitter, I., Neese, F., Costas, M., Ye, S., and Meyer, F. (2017). Nonclassical single-state reactivity of an oxo-iron(IV) complex confined to triplet pathways. *J. Am. Chem. Soc.* 139, 8939–8949.
85. Mondal, B., Neese, F., Bill, E., and Ye, S. (2018). Electronic structure contributions of non-heme oxo-iron(V) complexes to the reactivity. *J. Am. Chem. Soc.* 140, 9531–9544.
86. Ye, S., Geng, C.Y., Shaik, S., and Neese, F. (2013). Electronic structure analysis of multistate reactivity in transition metal catalyzed reactions: the case of C-H bond activation by non-heme iron(IV)-oxo cores. *Phys. Chem. Chem. Phys.* 15, 8017–8030.
87. Ray, K., George, S.D., Solomon, E.I., Wieghardt, K., and Neese, F. (2007). Description of the ground-state covalencies of the bis(dithiolato) transition-metal complexes from x-ray absorption spectroscopy and time-dependent density-functional calculations. *Chem. Eur. J.* 13, 2783–2797.
88. MacMillan, S.N., and Lancaster, K.M. (2017). X-ray spectroscopic interrogation of transition-metal-mediated homogeneous catalysis: primer and case studies. *ACS Catal.* 7, 1776–1791.
89. Wang, M., Weyhermüller, T., Bill, E., Ye, S., and Wieghardt, K. (2016). Structural and spectroscopic characterization of rhodium complexes containing neutral, monoanionic, and dianionic ligands of 2,2'-bipyridines and 2,2':6,2'-terpyridines: an experimental and density functional theory (DFT)-computational study. *Inorg. Chem.* 55, 5019–5036.
90. Wang, C.Y. (2013). Manganese-mediated C-C bond formation via C-H activation: from stoichiometry to catalysis. *Synlett* 24, 1606–1613.
91. Valyaev, D.A., Lavigne, G., and Lugan, N. (2016). Manganese organometallic compounds in homogeneous catalysis: past, present, and prospects. *Coord. Chem. Rev.* 308, 191–235.
92. Garbe, M., Junge, K., and Beller, M. (2017). Homogeneous catalysis by manganese-based pincer complexes. *Eur. J. Org. Chem.* 2017, 4344–4362.
93. Hu, Y.Y., Zhou, B.W., and Wang, C.Y. (2018). Inert C-H bond transformations enabled by organometallic manganese catalysis. *Acc. Chem. Res.* 51, 816–827.
94. Agapie, T., Schofer, S.J., Labinger, J.A., and Bercaw, J.E. (2004). Mechanistic studies of the ethylene trimerization reaction with chromium-diphosphine catalysts: experimental evidence for a mechanism involving metallacyclic intermediates. *J. Am. Chem. Soc.* 126, 1304–1305.
95. Overett, M.J., Blann, K., Bollmann, A., Dixon, J.T., Haasbroek, D., Killian, E., Maumela, H., McGuinness, D.S., and Morgan, D.H. (2005). Mechanistic investigations of the ethylene tetramerisation reaction. *J. Am. Chem. Soc.* 127, 10723–10730.
96. McGarry, K.R., and Vicic, D.A. (2017). A perfluorometallacycloheptane complex of nickel bipyridine. *J. Fluorine Chem.* 203, 206–209.
97. Montgomery, J. (2004). Nickel-catalyzed reductive cyclizations and couplings. *Angew. Chem. Int. Ed.* 43, 3890–3908.
98. Broene, R.D. (2007). Reductive coupling of unactivated alkenes and alkynes. *Top. Curr. Chem.* 279, 209–248.
99. Gandeepan, P., and Cheng, C.H. (2015). Cobalt catalysis involving π components in organic synthesis. *Acc. Chem. Res.* 48, 1194–1206.
100. Fürstner, A. (2016). Iron catalysis in organic synthesis: a critical assessment of what it takes to make this base metal a multitasking champion. *ACS Cent. Sci.* 2, 778–789.
101. Chirik, P.J. (2017). Carbon-carbon bond formation in a weak ligand field: leveraging open-shell first-row transition-metal catalysts. *Angew. Chem. Int. Ed.* 56, 5170–5181.
102. Carbonar, A., Cambisi, F., and Dall'Asta, G. (1971). Catalytic behavior of some Ziegler-Natta catalysts in norbornadiene-butadiene codimerization. *J. Org. Chem.* 36, 1443–1445.
103. Yang, T., and Ehara, M. (2017). Computational studies on reaction mechanism and origins of selectivities in nickel-catalyzed (2+2+2) cycloadditions and alkenylative cyclizations of 1,6-ene-allenes and alkenes. *J. Org. Chem.* 82, 2150–2159.
104. Brinkman, E.A., Berger, S., and Brauman, J.I. (1994). A-silyl-substituent stabilization of carbanions and silyl anions. *J. Am. Chem. Soc.* 116, 8304–8310.
105. Hoyt, J.M., Sylvester, K.T., Sernproni, S.P., and Chirik, P.J. (2013). Synthesis and electronic structure of bis(imino)pyridine iron metallacyclic intermediates in iron-catalyzed cyclization reactions. *J. Am. Chem. Soc.* 135, 4862–4877.
106. Hossain, M.A., Kim, H.S., Houk, K.N., and Cheong, M. (2014). Spin-crossover in chromium-catalyzed ethylene trimerization: density functional theory study. *Bull. Korean Chem. Soc.* 35, 2835–2838.
107. Bolig, A.D., and Brookhart, M. (2007). Activation of sp^3 C-H bonds with cobalt(II): catalytic synthesis of enamines. *J. Am. Chem. Soc.* 129, 14544–14545.
108. Hung-Low, F., Krogerman, J.P., Tye, J.W., and Bradley, C.A. (2012). Development of more labile low electron count Co(II) sources: mild, catalytic functionalization of activated alkanes using a $[(\text{Co}^{+}\text{Co})_2\text{-}\mu\text{-}(\text{I}^4\text{:}\text{I}^4\text{-arene})]$ complex. *Chem. Commun.* 48, 368–370.
109. Ozin, G.A., McCaffrey, J.G., and Parnis, J.M. (1986). Photochemistry of transition-metal atoms - reactions with molecular-hydrogen and methane in low-temperature matrices. *Angew. Chem. Int. Ed.* 25, 1072–1085.
110. Yasuda, H., Tatsumi, K., and Nakamura, A. (1985). Unique chemical behavior and bonding of early-transition-metal diene complexes. *Acc. Chem. Res.* 18, 120–126.
111. Cavell, K.J. (1996). Recent fundamental studies on migratory insertion into metal-carbon bonds. *Coord. Chem. Rev.* 155, 209–243.